Band structure in the neutron-rich lanthanide nucleus ^{152}Nd. II. Allowed and K-forbidden transitions from the negative-parity bands

M. Hellström, H. Mach, B. Fogelberg, D. Jerrestam, and L. Spanier
Department of Neutron Research, University of Uppsala, S-61182 Nyköping, Sweden
(Received 9 June 1992)

A fast timing $\beta\gamma\gamma(t)$ method has been used to measure level lifetimes in ^{152}Nd as populated in the β^- decay of ^{152}Pr. The following half-lives have been measured: $T_{1/2}$=330(14) and 53(10) ps for the 236.7 keV 4_1^+ and the 484.0 keV 6_1^+ members of the ground-state band, $T_{1/2}$=145(11), 12(7), and 64(56) ps for the 1542.0 keV 2^-, 1600.7 keV 3^-, and the 1683.2 keV 4^- members of the K^π=2^- band, and $T_{1/2}$=42(6) and 30(10) ps for the 1827.5 keV 3^- and the 1898.3 keV 4^- members of the K^π=3^- band, respectively. The observed allowed $M1$ rates and large hindrance factors for the $E1$ transitions deexciting these bands is discussed in terms of K forbiddenness and the (suggested) dominant two-quasiparticle configurations. Systematics of the octupole vibrational bands in the rare-earth region is examined. The energy minima for the K^π=1^- bands follow a narrow valley along $N = 94$ associated with the two-quasineutron $\{\nu 5/2^+[642] - \nu 3/2^-[521]\}$ configuration, while minima for the K^π=2^- bands follow narrow valleys at $Z = 66$ and $Z = 74$ associated with the two-quasiproton configurations $\{\pi 7/2^-[523] - \pi 3/2^+[411]\}$ and $\{\pi 9/2^-[514] - \pi 5/2^+[402]\}$, respectively. In contrast, the lowering of the K^π=0^- bands near ^{146}Ba is along both neutron and proton numbers, giving a flat minimum.

PACS number(s): 27.70.+q, 23.20.Gq, 23.20.Lv

I. INTRODUCTION

Although quadrupole and octupole vibrations represent the most basic modes of nuclear excitation [1], little is known about octupole excited states in contrast to the richness of data on quadrupole collectivity. The data on the negative parity states are particularly limited for the light neutron-rich lanthanides which are situated at the important intersection of two transitional regions: the transition from spherical to quadrupole deformed shapes at N=88/90 [2] and the transition from octupole vibrational excitations near ^{146}Gd [3] to the static octupole deformation (or strong softness towards octupole deformation) near ^{146}Ba [4]. These nuclei feature the lowest-lying 1_1^- states in the rare-earth region [1, 5] with the K^π=0^- excitations well below 800 keV in ^{148}Ce and $^{144-148}$Ba. The properties of these states show strong fluctuations. The $B(E1)$ branching ratios and the $B(E1)$ rates show abrupt changes in ^{146}Ba [4], while a sudden increase in excitation energy is observed for the K^π=0^- band in ^{152}Nd [5, 6].

Recent model refinements [7] allow one to study the combined effects of quadrupole and higher modes of excitation including the important interplay between the quadrupole and octupole modes. Any critical testing of such models requires extensive data on nuclear properties. Yet, in the case of the light neutron-rich lanthanides, the knowledge has been limited to the systematics of the lowest members of the K^π=0^- band [including some $B(E1)$ and $B(E3)$ rates]. Almost nothing is known about the (other) higher-lying bands although such data would provide essential constraints to the model predictions.

It is thus indeed fortunate that the odd-odd nuclei in the A = 140–160 region often have negative-parity ground states which, via the β^- decay, preferentially populate states with negative parity in their even-even daughter nuclei. This provides efficient means, and in fact a unique opportunity, to study the systematics of the negative-parity states of different types (including the octupole bands) in the light n-rich lanthanide region.

So far it has been difficult to access most of the neutron-rich nuclei in the A = 140–160 region, and furthermore no general method to measure lifetimes in the critical domain below 1 ns has been available for these nuclei. The introduction of a fast time-delayed coincidence method [8, 9] and the recent improvements of the target and ion source used at Studsvik [10, 11] have made it possible to overcome these problems.

The subject of this study is the band structure in ^{152}Nd. In part I of this work (see Ref. [12]) we have reported on the detailed γ-ray spectroscopy of levels in ^{152}Nd populated in the β^- decay of ^{152}Pr and have discussed the anomalous properties of the observed positive-parity bands. Our data, which include $\gamma\gamma(\theta)$ coincidences and γ-ray singles, have been combined with the results of the earlier studies on ^{152}Nd as populated in the β^- decay of ^{152}Pr (Karlewski *et al.* [6] and Hellström *et al.* [13]), in the spontaneous fission of ^{252}Cf [14, 15] and in the ^{150}Nd$(t,p)^{152}$Nd reaction [16]. A number of new γ transitions and energy levels as well as new spin and parity assignments have been established. In particular we have confirmed the assignment of two octupole bands, one with K^π=0^- and the other with K^π=2^- previously proposed [6] on the basis of the systematics of the N = 92 isotones and the branching ratios of the depopulating γ rays. The negative-parity bands identified in part I of our study [12] are illustrated in Fig. 1.

In the present paper, which represents part II of the study, we report the lifetime measurements in ^{152}Nd using the aforementioned $\beta\gamma\gamma(t)$ fast timing technique

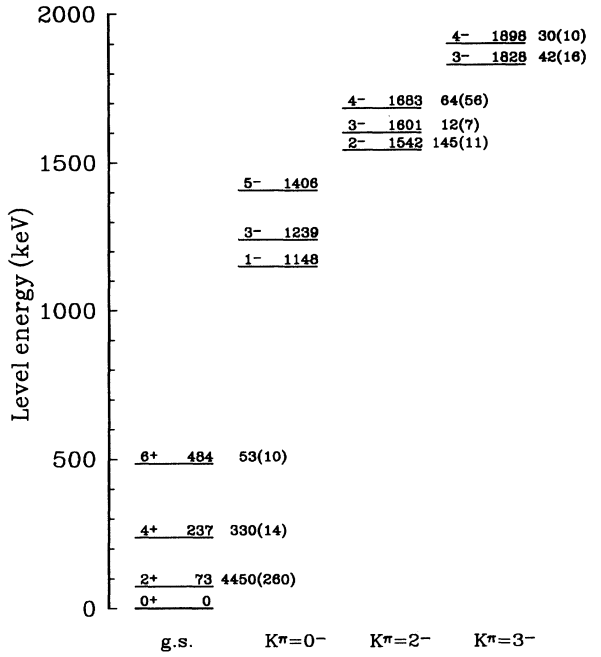

FIG. 1. Ground state and negative-parity $K^\pi = 0^-$, 2^-, and 3^- bands in ^{152}Nd identified in part I of this work [12]. The presently measured half-lives (in ps) are listed to the right of the level bars. The lifetime of the 2_1^+ state is from Ref. [13].

and elucidate on the properties of the negative-parity bands in ^{152}Nd. The present results complement our half-life measurement for the 2_1^+ state in ^{152}Nd reported in Ref. [13]. The experimental procedure is outlined in Sec. II below. The data analysis is presented in Sec. III, and a discussion of the results including properties of the negative-parity bands is given in Sec. IV.

II. EXPERIMENTAL DETAILS

The timing measurements were performed at the OSIRIS fission-product mass separator facility at Studsvik [10, 17, 18]. The source containing 1 g of ^{235}U was operated in the plasma ionization mode [10] at the temperature of ~2500 °C. The mass separated A=152 beam contained strong activities of ^{152}Pr, ^{152}Nd, and ^{152}Pm, including three known Pm isomers. The contamination of the beam by molecular ion species [19], such as carbides and dicarbides, was only marginal in this case. Lifetimes were measured using the triple coincidence $\beta\gamma\gamma(t)$ method detailed in Refs. [8, 9, 20, 21]. Only a brief account of the timing technique is given here.

Three detectors positioned in a plane around the direct beam collection point (parent port configuration) were used in the measurement. Lifetime information was derived from time-delayed $\beta\gamma$ coincidences in two fast timing detectors: a 2 mm Pilot-U plastic for β rays and a cylindrical BaF_2 crystal (with a diameter of 2.5 cm and a height of 2.5 cm) for γ transitions. The XP2020 and XP2020Q phototubes coupled to the Pilot-U plastic and BaF_2 crystal, respectively were operated in the anode mode [9]. The ΔE β detector provided a β response almost independent of the feeding β-ray energy, while an additional γ coincidence with a Ge detector was used to select the desired decay path. The BaF_2 crystal was strongly shielded from cross-scattered radiation by a combination of copper and lead absorbers. The overall fast timing resolution varied from the full width at half maximum (FWHM) of ~200 ps at $E_\gamma = 1$ MeV to about 300 ps at 250 keV. The $\beta\gamma\gamma(t)$ coincidence data were collected in cycles during deposition of the mass separated beam on a movable Al-covered Mylar tape. After 8 s of data collection the old source was removed before a new cycle began. Only events from the ^{152}Pr→^{152}Nd and ^{152}Pm→^{152}Sm decays were recorded as the β energy of the ^{152}Nd→^{152}Pm decay was too low to be accepted in the β gate. The results for ^{152}Sm are reported in a separate publication [22].

Data were collected onto the hard disk of a PC computer in quadruplets $(E_\gamma^{BaF_2}, \Delta E_\beta, E_\gamma^{Ge}, \Delta t_{fast})$ and sorted off line. The timing spectra were sorted with gates set on the full-energy peaks (and their respective backgrounds) in the BaF_2 and Ge detectors while a common gate was selected on the β spectrum. The subtraction of the Compton background from the full-energy peaks was made following procedures outlined in Ref. [20].

Lifetimes were measured by the centroid shift technique. The mean life τ ($\tau = T_{1/2}/\ln 2$) of a level directly β fed is given by the difference between the centroid of the delayed time spectrum and the prompt centroid of the same E_γ. In the case of indirect feeding (when the level of interest is fed by a γ ray from a higher-lying level) the mean life of interest is given by the difference between the centroid shift of the spectrum gated by the deexciting γ-ray and the shift of the spectrum gated by the feeding γ-transition.

Crucial to the centroid shift technique is the calibration of the prompt position as a function of γ-ray energy. The prompt and delayed time spectra were measured concurrently in order to maintain identical conditions in the face of small but persistent drifts of the electronics. However, since these internal prompt points were insufficient to map the prompt curve in the whole range of interest additional information was required. It was already verified [9, 20, 21] that the shape of the prompt curve is not affected by the electronic drifts although its position is shifted by a constant. The shape of the prompt curve (so-called "relative prompt" or "walk curve") is deduced in a dedicated calibration measurement and is then shifted by a constant to overlap with prompt points internal to the decay under study. A relative prompt curve was deduced using a simple calibration procedure of Ref. [21] already applied to a number of measurements in the low-picosecond range [4, 23]. We performed a separate calibration measurement using the mass separated A = 96 beam as the decay schemes of ^{96}Rb→^{96}Sr and ^{96}Sr→^{96}Y are simple and the lifetimes of several key levels in ^{96}Sr and ^{96}Y have recently been measured [21] with high precision.

The constant by which the relative prompt curve had to be shifted to overlap with the prompt points internal to the ^{152}Pr→^{152}Nd decay was obtained by using the centroid positions of time spectra assumed to be

prompt. These spectra were obtained by setting gates on the Compton tails of high-energy transitions which deexcite higher-lying levels with $E \geq 2$ MeV and feed the level at 236.7 keV.

III. DATA ANALYSIS

In general the new lifetime results, which are listed in Table I, represent averages over a few independent results obtained by selecting, for example, different transitions deexciting the same level or using different methods as discussed below. (The lifetime of the 72.6 keV level, taken from Ref. [13], was deduced from a slope fitting rather than from a centroid shift analysis.) In particular, the mean lives of the levels at 484.0, 1827.5, and 1898.3 keV were deduced directly by observing shifts of their delayed time spectra relative to the prompt position, τ_0. No corrections were made for any indirect γ feeding. Such corrections would be small for the levels at ≈ 1.8 MeV which are fed by strong β transition, but could be significant for the level at 484.0 keV. As no correction can be presently assessed for this level, none was made. However, such a correction of the half-life, though plausible, should not exceed a value of 5 ps (which is well within the quoted uncertainty of ± 10 ps). This limit on the correction has been estimated by comparing the quadrupole moments deduced for the 2_1^+ and 4_1^+ states to the value deduced for the 6_1^+ state at 484.0 keV and assuming a constant quadrupole moment for the ground-state (g.s.) rotational band in ^{152}Nd (see discussion in Sec. IV A). The lifetimes of the levels at 1827.5 and 1898.3 keV represent an average of five and two independent results, respectively, while the lifetime of the 484.0 keV level was deduced from a single result.

TABLE I. Level lifetimes in ^{152}Nd deduced in the present study.

Level (keV)	$T_{1/2}$ (ps)	Centroid shift analysis[a]
72.6	4450(260)[b]	
236.7	330(14)	(73–164)-τ_0-FFA
		(247–164)-(164–247)
		(298–164)-(298–1364)
		(1364–164)-(164–1364)
484.0	53(10)	(164–247)-τ_0
1542.0	145(11)	(285–291)-ACS(1827)
		(285–393)-ACS(1827)
		(285–1470)-ACS(1827)
1600.7	12(7)	(164–1364)-FFA
		(226–1364)-ACS(1827)
		(298–1364)-ACS(1898)
1683.2	64(56)	(215–164)-ACS(1898)-τ_{237} [c]
1827.5	42(6)	(291–285)-τ_0
		(303–285)-τ_0
		(393–285)-τ_0
		(1364–227)-τ_0
		(1470–285)-τ_0
1898.3	30(10)	(1364–298)-τ_0
		(1446–215)-τ_0

[a]Notation: $(A-B)$ — a timing spectrum used in the centroid shift analysis labeled by A and B which indicate the energy in keV of the gating transitions in the Ge and in the BaF_2 detectors, respectively; τ_0 — position of the prompt; FFA — correction for the time delay brought by the indirect γ feeding from above; ACS(C) — the average centroid shift of the transition directly feeding from above and deexciting level C.

[b]From Ref. [13].

[c]Correction for the mean life of the 236.7 keV level.

The lifetimes of the remaining levels were deduced by a relative shift technique in which the mean life is obtained as the difference between the centroid shift of the transition deexciting the level of interest and the centroid shift of a transition directly feeding this level. These results are the most reliable as they do not depend on the absolute prompt normalization, but only on the shape of the prompt curve ("relative prompt" or a "walk curve"). The lifetimes of the levels at 1600.7, 236.7, and 1683.2 keV were deduced (in that order) at the end of the analysis as the analysis of their time spectra required corrections for the lifetimes of other levels. The lifetimes for the 236.7, 1542.0, and 1600.7 keV levels were averaged over four, three, and three independent results, respectively. The lifetime of the level at 1683.2 keV is based on a single result which also necessitated more elaborate corrections.

When the fast timing FWHM resolution is ~ 100 ps, a half-life longer than 30–40 ps manifests itself as a visible slope on the delayed part of the time spectrum [9]. Our timing resolution is about 2 times lower than that obtained in Ref. [9], thus only half-lives longer than $\sim$80 ps would show as clearly visible slopes. Figure 2 shows three time-delayed spectra related to the half-lives of 42, 145, and 330 ps of the levels at 1827.5, 1542.0, and 236.7 keV, respectively. The spectra of Fig. 2 confirm the relatively long lifetimes measured for the latter levels. The top panel shows a time spectrum obtained by gating on the feeding β transition as "start" and the 285.0 keV γ ray in the BaF_2 crystal as "stop," with an additional gate set on the 1469.5 keV γ ray in the Ge detector. The half-life of the 1827.5 keV level, $T_{1/2}$=42(16) ps, is too short to be visible as a slope on the delayed side of the spectrum. However, by "reversing" the gate by setting gates on the 285.0 keV transition in the Ge detector and on the 1469.5 keV γ ray in the BaF_2 detector, a visible slope on the delayed side is obtained due to the half-life of $T_{1/2}$=145(11) ps of the 1542.0 keV level, see the middle panel. In the bottom panel, the slope due to the longer half-life of $T_{1/2}$=330(14) ps of the level at 236.7 keV is even more pronounced.

In the case illustrated in the middle panel of Fig. 2, the time spectrum represents a convolution of two half-lives: 42(6) ps for the 1827.5 keV level and 145(11) ps for the level at 1542.0 keV. The quality of the data is not sufficient to separate these half-lives with a precision better than that provided by the centroid shift analysis. Due to weak statistics, the spectrum in the bottom panel represents the sum of two timing spectra obtained by setting gates on the 226.7 and 297.6 keV γ rays in the Ge detector, respectively, using a common gate on

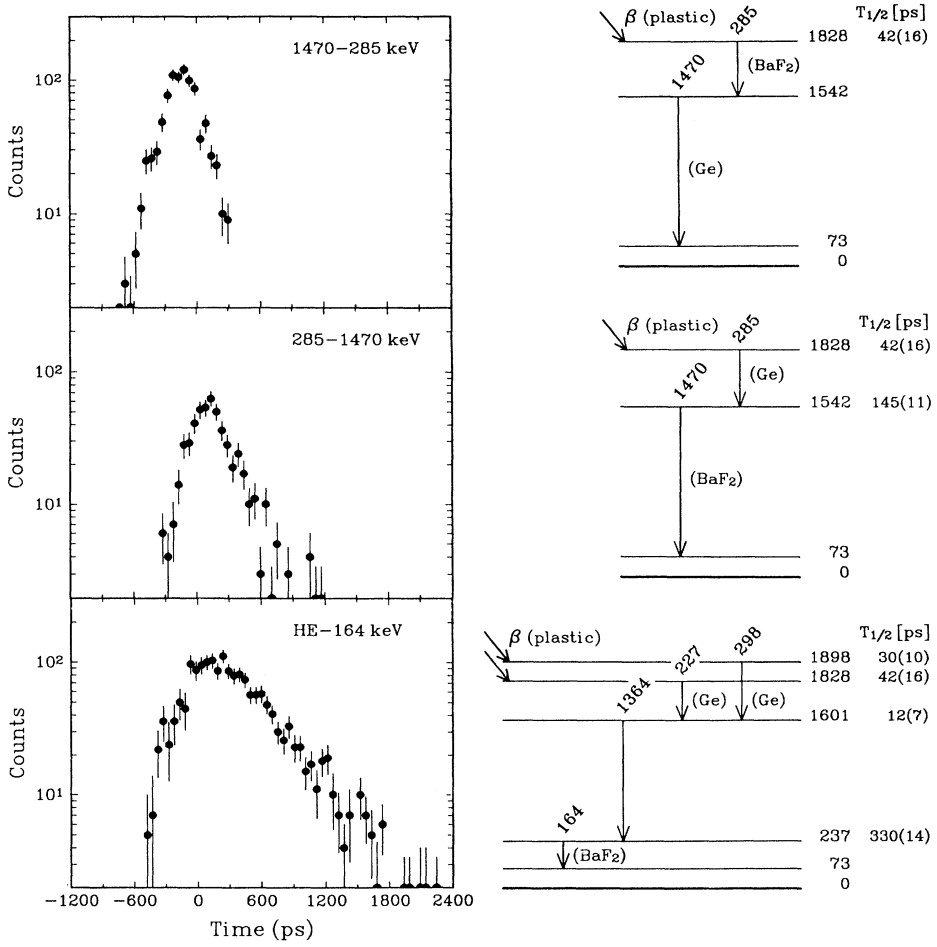

FIG. 2. Three time-delayed coincidence spectra illustrating the quality of the timing results. To the right of each timing spectrum is a partial level scheme incorporating the transitions involved, indicating the gating procedure and the half-lives (in ps) of the pertinent levels. The top panel illustrates the time distribution obtained by setting gates on the 1470 (Ge) and 285 keV (BaF_2) transitions. Because of the short lifetime of the 1827.5 keV level, $T_{1/2}$ = 42 ps, no slope is visible. The middle panel shows the "reversed" gate which has a visible slope due to the $T_{1/2}$ = 145 ps lifetime of the 1542.0 keV level. The time distribution in the bottom panel exhibits a significant slope due to the long half-life, $T_{1/2}$ = 330 ps of the 236.7 keV level. See the text for details.

the 164.1-keV transition in the BaF_2 detector and a common β gate. Each of these carry different (although much shorter) time-delayed components from higher-lying levels which, in this case too, makes slope fitting much less precise than the centroid shift analysis.

IV. BAND STRUCTURE OF ^{152}Nd

A. The ground-state band

The ground-state band, which has been identified [15, 16] up to the $I = 8$ level, shows the regular features of a rotational band characteristic of a strongly deformed nucleus. The excitation energy of the 2_1^+ state is among the lowest in the rare-earth region [5] which, along with a few other properties of the positive-parity bands, indicate unusual features of ^{152}Nd. These features, highlighted by the anomalous properties of the excited $K^\pi=0^+$ band, have been discussed in part I of this study [12].

The lifetime of the 2_1^+ level in ^{152}Nd has recently been measured [13] for the first time. The result of $T_{1/2}$=4.45(26) ns removed [13] a significant deviation at ^{152}Nd in the $B(E2)$ systematics [24] for the neutron-rich Nd isotopes. We note that the half-life of 7.7(20) ns adopted in the compilation of Ref. [24] for the 2_1^+ level in ^{152}Nd was in fact a tentative value measured for the nucleus of ^{154}Nd by Jared *et al.* [25] and reassigned by the compilers to ^{152}Nd.

The new results reported in this study extend the lifetime information on the g.s. band to the $I = 6$ level, see Table I. From the measured $B(E2)$ rates one can deduce values for the intrinsic quadrupole moment Q_0 of 6.22(20), 6.05(13), and 5.76(56) b for the 2_1^+, 4_1^+, and 6_1^+ band members, respectively. These values agree within the uncertainty limits with the assumption of a constant intrinsic quadrupole moment as expected for the rotational band. The average value for such a Q_0 moment is 6.09(11) b.

B. The $K^\pi=2^-$ and $K^\pi=3^-$ bands and the ^{152}Pr ground state

Based on the experimental data, one can identify two bands with $K = 2$ and 3 with bandheads at 1542.0 and 1827.5 keV, respectively. The transition probabilities deduced from the level half-lives listed in Table I are only compatible with a negative parity assignment to these bands. The strong β feeding to the 3^- and 4^- members of the $K = 3$ band, with logft= 4.9 and 5.4, respectively, is in agreement with the Alaga rule [26] for choices of $KI^\pi=33^-$ or 44^- of the ^{152}Pr β-decaying ground state. Accepting the conclusions of Sood and

Sheline [27] regarding the nature of allowed unhindered β transitions in this region leads to the 4^- alternative being the only realistic one. The reason is that the β transition must take place between configurations involving the $3/2^-[532]$ neutron and the $5/2^-[532]$ proton, as well as spectator neutrons, the configuration of which remains unchanged. Consequently, the β transition must feed a level of lower spin. (A 3^- ground state of ^{152}Pr would therefore predominantly populate a $KI^\pi=22^-$ state in ^{152}Nd, which is contrary to our observations.)

The lowest-lying states with a negative parity are often taken to represent collective octupole vibrations, although both theoretical [28] and experimental [5] works show that these states are often completely dominated by specific two-quasiparticle states. Such feature could naturally be present in the $K^\pi=2^-$ and $K^\pi=3^-$ bands since their excitation energies are at or above the pairing energy gap of $\sim$1.5 MeV. Some insight in the microscopic composition of the negative-parity states of ^{152}Nd can be obtained simply by an examination of the orbitals near the Fermi surface, see Table II. The β-decay properties discussed above allow the conclusion that the main component of the 3^- level at 1827.5 keV is, see Table II, the $\{\nu 3/2^-[532] + \nu 3/2^+[651]\}$ two-quasiparticle state. Likewise, one can expect the 2^- state at 1542.0 keV to have a large amplitude of $\{\nu 3/2^-[532] + \nu 1/2^+[660]\}$. The $M1$ transitions between members of the $K^\pi=3^-$ and 2^- bands are then essentially of the $\nu 3/2^+[651] \rightarrow \nu 1/2^+[660]$ type, and thus allowed. This is reflected by the low hindrance factors of $F_W \approx 100$ for these transitions, see Table III. Hindrance factors of this magnitude are generally found for allowed $M1$ transitions in odd-mass deformed nuclei. Meyer *et al.* [31] have reported a similar value ($F_W=67$) for an $M1$ transition between two two-quasiparticle states in ^{168}Er. The work of Meyer *et al.* also yielded rates for the K-forbidden $E1$ transitions to the ground-state band from the $K^\pi=3^-$ state in the same nucleus. The corresponding transitions in ^{152}Nd, see Table III, are about 1 order of magnitude slower than in ^{168}Er, where the hindrance factors F_W range from 2.0×10^6 to 2.0×10^7.

TABLE II. Nilsson orbitals expected near the Fermi surface in ^{152}Nd and low-lying two-quasiparticle states with negative parity.

Orbital		Two-quasiparticle states[a]	
Protons			
$P1$	$3/2^+[411]$	$K=0^-$	...
$P2$	$5/2^+[413]$	$K=1^-$	$P1$–$P3$
$P3$	$5/2^-[532]$	$K=2^-$	$P3$–$P5$
$P4$	$3/2^-[541]$	$K=3^-$	...
$P5$	$9/2^+[404]$		
Neutrons			
$N1$	$5/2^-[523]$	$K=0^-$	$N3-N5$, $N4-N7$
$N2$	$5/2^+[642]$	$K=1^-$	$N2-N3$, $N4-N5$
$N3$	$3/2^-[521]$	$K=2^-$	$N6+N7$, $N2-N4$
$N4$	$1/2^-[530]$	$K=3^-$	$N1+N7$, $N5+N6$
$N5$	$3/2^+[651]$		
$N6$	$3/2^-[532]$		
$N7$	$1/2^+[660]$		

[a]Only levels expected at low energies are given, see the coupling rule of Gallagher [29] and the systematics of Sood, Headly, and Sheline [5].

Despite the two-quasineutron nature of the $K^\pi=3^-$ band, it is still worthwhile to look for the vibrational strength. Although we have not been able to determine a definite transition rate for the $E3$ transition deexciting the 3^- level at 1827.5 keV, our upper limit of $B(E3) \leq 3$ Weisskopf units (W.u.) shows a rather low collectivity. In general, collective $B(E3)$ rates vary strongly with the quadrupole deformation of the core [32] and range from about 35–45 W.u. for vibrational nuclei like ^{146}Gd, to about 2–4 W.u. for deformed nuclei like ^{168}Er. Furthermore, these rates are usually the highest for the lowest-lying 3^- states and may decrease for the higher-lying states. These features are well reproduced by the random-phase-approximation calculations [28].

C. The $K^\pi=0^-$ and $K^\pi=1^-$ bands

The theoretical work of Neergård and Vogel [28] shows an ordering of the octupole states with increasing energy for increasing values of K in the $A \approx 150$ region. The simple considerations given in Table II suggest that several configurations are present that may give rise to relatively low-lying $K^\pi=0^-$ and 1^- states. We observe levels at 1148.4, 1238.5, and 1406.0 keV that are highly likely to represent the 1^-, 3^-, and 5^- members of a $K^\pi=0^-$ band. The $E1$ branching of the transitions to the ground-state band is in good agreement with the Alaga rule for $K=0$, but differs markedly from the branching pattern expected for $K=1$. The two lower band members were observed by Karlewski *et al.* [6] who also suggested that these levels belong to a $K^\pi=0^-$ band.

Our data give no indications for any low-lying levels having the decay characteristics of a $K^\pi=1^-$ band. Such a band, if present below the $K^\pi=2^-$ band by only $\sim$100 keV, would be populated indirectly by γ rays from the $K^\pi=2^-$ band. On the other hand, if present in close vicinity of the $K^\pi=2^-$ band, it would manifest itself through perturbations of the $K^\pi=0^-$ and $K^\pi=2^-$ bands [1]. The level energies of these latter bands are in reasonable agreement with the rotational energy formula, but show in both cases a slight depression, of the

order of 2 keV, of the 3^- band member. This may indicate the presence of $\Delta K=1$ mixing of both bands with a higher-lying $K^\pi=1^-$ band. The mixing of the 3^- levels can be reinforced by successive $\Delta K=1$ admixtures of the $K^\pi=0^-$ and $K^\pi=2^-$ bands or by the possibility that the 3^- level of the (hypothetical) $K^\pi=1^-$ is the lowest in this band.

Any band mixing effects will manifest themselves strongly by affecting the hindrance for the γ decay of the $K^\pi=2^-$ band members. All these transitions are K forbidden and therefore have vanishing first-order transition matrix elements. The finite transition probabilities actually observed in these cases are generally thought [33] to mainly be a result of band mixing through Coriolis coupling ($\Delta K=1$) effects. The admixed amplitudes need not be the same for all band members. A substantial even-odd effect has been observed [34, 35] for, e.g., the negative-parity bands of ^{156,158}Gd. In the present case of ^{152}Nd, the data in Table III indeed show a substantial transition rate of the $KI^\pi = 23^- \rightarrow 03^-$ interband $M1$ transition, and also a relaxation of the hindrance of other K-forbidden transitions as compared with the γ decay of the even spin members of the $K^\pi=2^-$ band.

One should remember that the absolute transition rates out of the $KI^\pi=23^-$ level still are small on an absolute scale, although they are large compared to those of the even spin levels. A $\Delta K=1$ component of a few percent in the 3^- state is sufficient to explain the reduction in the hindrance factors shown in Table II. Such a small value, as well as the minor distortion of the level energies, suggest that the unobserved $K^\pi=1^-$ band is present well above the $K^\pi=2^-$ bandhead.

D. Systematics of the octupole vibrational bands in the A =150 region

So far the data on the negative-parity states in the A =150 region have been too scarce to permit any meaningful systematic study [5]. Yet, the new systematics display a few interesting features and expose regions in

TABLE III. Hindrance factors for transitions from negative-parity states in ^{152}Nd.

Initial level		Final level	Gamma transition		
E_{level} (keV)	$T_{1/2}$ (ps)	KI^π	E_γ (keV)	Multipolarity[a]	F_W [b,c]
$K = 2^-$ band					
1542.0	145(11)	02^+	291.0	$E1$	2.6×10^5
($I^\pi = 2^-$)		03^-	302.8	$M1$	3.7×10^3
		01^-	393.3	$M1$	4.1×10^3
		02^+	1469.5	$E1$	2.5×10^6
		00^+	1541.8	$M2$	$>10^2$
1600.7	12(7)	02^+	350.5	$E1$	5.4×10^4
($I^\pi = 3^-$)		03^-	361.5	$M1$	4.3×10^2
		04^+	1363.8	$E1$	1.6×10^5
		02^+	1529.1	$E1$	2.3×10^6
1683.2	64(56)	22^-	141.9	$E2$	1.7×10^{-3}
($I^\pi = 4^-$)		04^+	1446.4	$E1$	1.2×10^6
$K = 3^-$ band					
1827.5	42(6)	24^-	144.5	$M1$	2.6×10^2
($I^\pi = 3^-$)		23^-	226.7	$M1$	1.2×10^2
		22^-	285.0	$M1$	6.5×10^1
		04^+	1591.0	$E1$	1.2×10^8
				($M2$	7.0×10^1)
		02^+	1754.5	$E1$	$> 1.0\times10^8$
				($M2$	$> 6.0\times10^1$)
		00^+	1827.1	E3	$> 3\times10^{-1}$
1898.3	30(10)	24^-	214.9	$M1$	4.4×10^1
($I^\pi = 4^-$)		23^-	297.6	$M1$	6.9×10^1
		04^+	1661.6	$E1$	7.9×10^6
				($M2$	4×10^0)
		02^+	1825.6	$M2$	$> 1.0\times10^1$

[a]The multipolarities have been deduced from the decay scheme, see Ref. [12].
[b]The hindrance factors are relative to the Weisskopf single-particle estimate [30].
[c]The uncertainties in the hindrance factors are proportional to those of the corresponding half-lives.

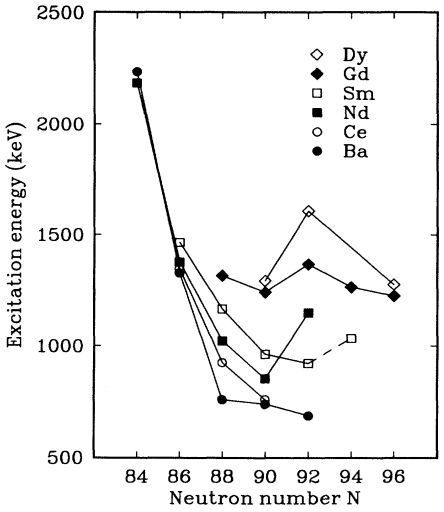

FIG. 3. Excitation energies of the $K^\pi=0^-$ bands in the $A=150$ region. Data for a given element are connected by a solid line. A tentative point for ^{156}Sm (see text) is connected to the rest of Sm systematics by a dashed line. Note the two characteristic features: a flat minimum near ^{146}Ba ($N=90$) as a function of both neutron and proton numbers, and an abrupt increase in excitation energy for ^{152}Nd ($N = 92$).

need of further studies.

The $K^\pi=0^-$ systematics of Fig. 3 shows a rather smooth and gradual decrease of the excitation energies with both increasing neutron and decreasing proton numbers towards a minimum near $^{146-148}$Ba (N =90–92). A singular departure from the smooth systematics appears at ^{152}Nd (N=92) where a sharp jump by ~300 keV is noticed. The N=92 systematics, plotted in Fig. 4, seems more difficult to interpret. At first it appears that the Sm point (Z = 62) is displaced from a smooth systematic trend, but on the other hand a curve could also be drawn through the data points for Z =56, 62, 64, and 66, making the Nd point (Z=60) show a sharp jump in energy. These conflicting interpretations may be resolved as new data become available. The excitation energy for ^{156}Sm (N=94), see Fig. 3, also appears to be low. [This point represents a tentative value obtained by subtracting from the energy of the 3^- state (suggested to be a member of the $K^\pi=0^-$ band [36]) the energy of 76 keV.]

In the $K^\pi=1^-$ systematics (Fig. 5), we observe a sharp lowering along a narrow valley at neutron number N=94 associated with the two-quasineutron $\{\nu 5/2^+[642] - \nu 3/2^-[521]\}$ configuration [5]. The $K^\pi=1^-$ band in ^{156}Sm, which we have tentatively identified [36] at the excitation energy of 803.5 keV, represents the lowest-lying $K^\pi=1^-$ band known in the rare-earth region [5]. However, as the minimum in the systematics of the $K^\pi=1^-$ bands has not been established, it is possible that the energy of this band is even lower in ^{154}Nd. This could explain the sudden rise of the $K^\pi=0^-$ band in ^{152}Nd (a trend that should also continue into ^{154}Nd if the following logic is true). A sharp minimum can occur only if the occupation of a specific quasiparticle configuration is optimal. Consequently, the minima in the excitation energies for bands with different K^π will be anticorrelated. Thus, lowering the $K^\pi=1^-$ band requires the $K^\pi=0^-$ band to rise in excitation energy since it is not likely to find optimal conditions for both excitations in the same nucleus.

In the $K^\pi=2^-$ systematics of Fig. 6, the excitation energies show a sharp lowering along two narrow valleys at proton numbers Z=66 (dysprosium) and Z =74 (tungsten) associated with the two-quasiproton $\{\pi 7/2^-[523] - \pi 3/2^+[411]\}$ and $\{\pi 9/2^-[514] - \pi 5/2^+[402]\}$ configurations, respectively [5].

In summary, the systematics of the $K^\pi=1^-$ and 2^- bands show rather similar features that contrast with the pattern of the $K^\pi=0^-$ excitations. In both cases, one observes a sharp lowering of the excitation energies

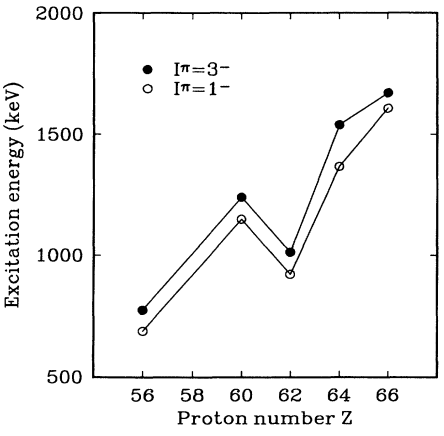

FIG. 4. Excitation energies of the $I^\pi=1^-$ and 3^- members of the $K^\pi=0^-$ bands at N = 92. Note that depending on what trend one expects the systematics to follow, it is either the Sm point (Z=62) or the Nd one (Z=60) that appears to be abruptly displaced from the otherwise smooth systematics. The presently unknown data points for ^{150}Ce could clarify the situation.

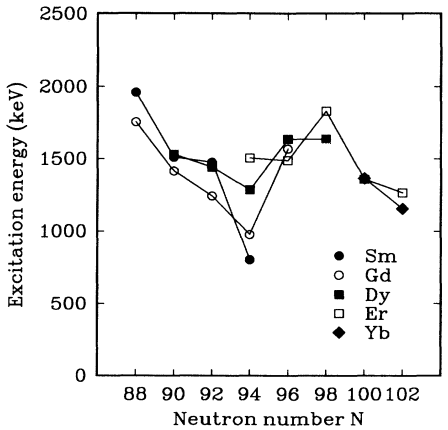

FIG. 5. Excitation energies of the $K^\pi=1^-$ bands in the $A=150$ region. Data for a given element are connected by a solid line. A narrow lowering of the energies along the N=94 valley is clearly visible.

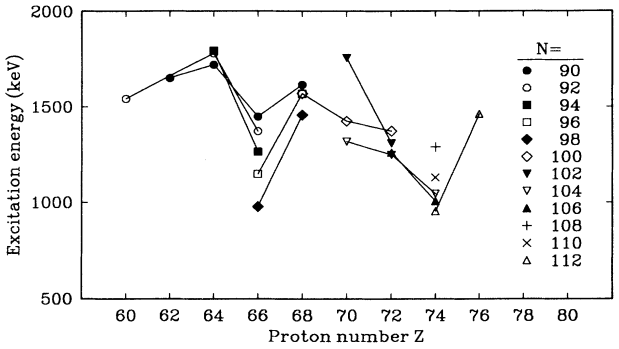

FIG. 6. Excitation energies of the $K^\pi=2^-$ bands in the A=150 region. For each isotonic chain the data have been connected by a solid line. A narrow lowering of the energies along the $Z=66$ (dysprosium) and $Z=74$ (tungsten) valleys are well visible.

along well-defined neutron or proton numbers, indicating strong influence of the specific quasiparticle contributions. (In contrast, the lowering of the $K^\pi=0^-$ bands is along both neutron and proton numbers, giving a flat minimum.) However, as the minimum excitation energy is well below 1 MeV, it needs to be explained why the quasiparticle configurations should have such a profound influence on the excitation energies at energies as low as half the pairing energy gap.

Our $B(E1;\ 1^- \rightarrow 0^+)/B(E1;\ 1^- \rightarrow 2^+)$ and $B(E1;\ 3^- \rightarrow 2^+)/B(E1;\ 3^- \rightarrow 4^+)$ branching ratios of 0.5 and 0.7, respectively, that were measured for the $K^\pi=0^-$ band in ^{152}Nd, compare closely with both the typical experimental values of 0.5 and 0.9, respectively, for the $K^\pi=0^-$ bands in the neutron-rich Ba-Gd nuclei, and the theoretical ratios based on the Alaga rules of 0.5 and 0.75, respectively. It should be noted that the experimental ratios remain fairly constant in this region with the notable exception of ^{146}Ba, where both of these ratios drop to the value of 0.11 [4]. This nucleus also experiences a sudden drop in the absolute $B(E1)$ rates [4] that is of a considerable theoretical interest [4, 37].

Although the systematics of the $B(E1)$ branchings for the $K^\pi=1^-$, 2^-, and 3^- bands is scarce some strong differences for the neighboring nuclei are visible. (One should be cautious with the unusual branchings as it is difficult to provide reliable intensities for the weak and overlapping γ lines.) For the $K^\pi=2^-$ band in ^{152}Nd, our $B(E1;\ 3^- \rightarrow 2^+)/B(E1;\ 3^- \rightarrow 4^+)$ branching ratio of 0.07 is an order of magnitude lower than the average value of ~0.6 for the Ba-Gd nuclei. Compare, e.g., with the values of 0.12 for ^{152}Sm and 1.4 for ^{156}Gd.

The systematics of the A =150 mass region discussed in this section indicate that the excitation energies and the branching ratios of the octupole vibrational bands show strong local variations presumably due to specific two-quasiparticle contributions. Such strong local changes cannot be explained in the models where the microscopic composition is not explicitly taken into account.

V. SUMMARY AND CONCLUSIONS

Recent improvements to the ion source at OSIRIS have made it possible to provide intense beams of ^{152}Pr which in turn allowed detailed study of the ^{152}Pr→^{152}Nd decay. We have firmly identified the $K^\pi=0^-$ and $K^\pi=2^-$ bands in ^{152}Nd and confirmed the tentative identification of the first two members of each band suggested by Karlewski *et al.* [6]. The higher sensitivity of our γ-branching data [12] has allowed us to locate further members of these excited bands and to identify a $K^\pi=3^-$ band at higher excitation energy.

In this study, which represents the first application of the $\beta\gamma\gamma(t)$ fast timing method at OSIRIS, we report the results of lifetime measurements for the following levels: the g.s. band up to and including the $I = 6$ level, the first three members of the $K^\pi=2^-$ band, and the first two members of the $K^\pi=3^-$ band. The deduced $E1$ transition rates show strong hindrance and confirm the proposed K assignments. On the other hand, allowed $M1$ rates combined with the pattern of two allowed unhindered β transitions permitted us to identify the major structural components in terms of two-quasiparticle configurations for the observed negative-parity bands and for the β-decaying state of ^{152}Pr. The suggested dominant two-quasiparticle configurations are $\{\pi 5/2^-[532] + \nu 3/2^+[651]\}$ for the g.s. of ^{152}Pr and $\{\nu 3/2^-[532] + \nu 3/2^+[651]\}$ for the $K^\pi=3^-$ band, while the $K^\pi=2^-$ band has a large component of the $\{\nu 3/2^-[532] + \nu 1/2^+[660]\}$ two-quasiparticle configuration. There is some evidence for $\Delta K=1$ mixing in the $K^\pi=0^-$ and $K^\pi=2^-$ bands, although we could not identify any levels of a $K^\pi=1^-$ band. As a result of the present study, ^{152}Nd represents the first light neutron-rich lanthanide nucleus which octupole bands, including transition rates, are fairly well known, and thus amenable to critical model testing.

Such models, however, must explicitly include the microscopic composition of a nucleus. This need is clearly seen in the energy systematics of the octupole vibrational bands where the energies of the $K^\pi=1^-$ and 2^- bands show strong sensitivity to specific quasiparticle occupation. The minima in the excitation energies of the octupole bands have not yet been established, but for the $K^\pi=0^-$ and 1^- bands these are expected to occur in the neutron-rich light lanthanides.

ACKNOWLEDGMENTS

The assistance of Leif Jacobsson and Olof Johansson in operating the mass separator is gratefully acknowledged. This work was supported by the Swedish Natural Science Research Council.

[1] S. Rohoziński, Rep. Prog. Phys. **51**, 541 (1988), and references therein.
[2] K. Kumar, Nucl. Phys. A **231**, 189 (1974), and references therein.
[3] P. Kleinheiz, Phys. Scr. **24**, 236 (1981).
[4] H. Mach, W. Nazarewicz, D. Kusnezov, M. Moszyński, B. Fogelberg, M. Hellström, L. Spanier, R. L. Gill, R. F. Casten, and A. Wolf, Phys. Rev. C **41**, R2469 (1990), and references therein.
[5] P. C. Sood, D. M. Headly, and R. K. Sheline, At. Data Nucl. Data Tables **47**, 89 (1991).
[6] T. Karlewski, N. Hildebrand, M. Brugger, N. Kaffrell, N. Trautmann, and G. Herrmann, Z. Phys A **330**, 55 (1988).
[7] S. Ćwiok and W. Nazarewicz, Nucl. Phys. A **496**, 367 (1989), and references therein.
[8] H. Mach, R. L. Gill, and M. Moszyński, Nucl. Instrum. Methods **A280**, 49 (1989).
[9] M. Moszyński and H. Mach, Nucl. Instrum. Methods **A277**, 407 (1989).
[10] L. Jacobsson, B. Fogelberg, B. Ekström, and G. Rudstam, Nucl. Instrum. Methods Phys. Res. B **26**, 223 (1986).
[11] B. Fogelberg, M. Hellström, L. Jacobsson, D. Jerrestam, L. Spanier, and G. Rudstam, Nucl. Instrum. Methods Phys. Res. B **70**, 137 (1992).
[12] M. Hellström, B. Fogelberg, H. Mach, D. Jerrestam, and L. Spanier, Phys. Rev. C **46**, 860 (1992).
[13] M. Hellström, H. Mach, B. Fogelberg, D. Jerrestam, and L. Spanier, Phys. Rev. C **43**, 1462 (1991).
[14] C. M. Baglin, Nucl. Data Sheets **30**, 1 (1980).
[15] J. B. Wilhelmy, S. G. Thompson, R. C. Jared, and E. Cheifetz, Phys. Rev. Lett. **25**, 1122 (1970).
[16] R. Chapman, W. McLatchie, and J. E. Kitching, Nucl. Phys. A **186**, 603 (1972).
[17] S. Borg, I. Bergström, G. B. Holm, B. Rydberg, L.-E. DeGeer, G. Rudstam, B. Grapengiesser, E. Lund, and L. Westgaard, Nucl. Instrum. Methods **91**, 109 (1971).
[18] G. Rudstam, Nucl. Instrum. Methods **139**, 239 (1976).
[19] M. Hellström, B. Fogelberg, L. Jacobsson, L. Spanier, and G. Rudstam, Nucl. Instrum. Methods Phys. Res. B **70**, 142 (1992).
[20] H. Mach, F. K. Wohn, G. Molnár, K. Sistemich, John C. Hill, M. Moszyński, R. L. Gill, W. Krips, and D. S. Brenner, Nucl. Phys. A **523**, 197 (1991).
[21] H. Mach, M. Moszyński, and R. L. Gill (unpublished).
[22] H. Mach, M. Hellström, B. Fogelberg, D. Jerrestam, and L. Spanier, Phys. Rev. C **46**, 1849 (1992).
[23] H. Mach, F. K. Wohn, M. Moszyński, R. L. Gill, and R. F. Casten, Phys. Rev. C **41**, 1141 (1990).
[24] S. Raman, C. H. Malarkey, W. T. Milner, C. W. Nestor, Jr., and P. H. Stelson, At. Data Nucl. Data Tables **36**, 1 (1987).
[25] R. C. Jared, H. Nifenecker, E. Cheifetz, J. B. Wilhelmy, and S. G. Thompson (private communication), quoted in Ref. [24].
[26] G. Alaga, K. Alder, A. Bohr, and B. R. Mottelson, Kgl. Dan. Vidensk. Selsk. Mat. Fys. Medd. **29**, No. 9 (1955).
[27] P. C. Sood and R. K. Sheline, At. Data Nucl. Data Tables **43**, 259 (1989).
[28] K. Neergård and P. Vogel, Nucl. Phys. A **145**, 33 (1970).
[29] C. J. Gallagher, Nucl. Phys. **16**, 215 (1960).
[30] J. M. Blatt and V. F. Weisskopf, *Theoretical Nuclear Physics* (Wiley, New York, 1952), p. 627.
[31] R. A. Meyer, D. R. Nethaway, A. L. Prindle, and R. P. Yaffe, Phys. Rev. C **35**, 1468 (1987).
[32] R. H. Spear, At. Data Nucl. Data Tables **42**, 55 (1989).
[33] A. Bohr and B. R. Mottelson, *Nuclear Structure* (Benjamin, Reading, 1975) Vol. II, Chap. 4.
[34] R. C. Greenwood *et al.*, Nucl. Phys. A **304**, 327 (1978).
[35] A. Bäcklin *et al.*, Nucl. Phys. A **380**, 189 (1982).
[36] M. Hellström, B. Fogelberg, L. Spanier, and H. Mach, Phys. Rev. C **41**, 2325 (1990).
[37] P. A. Butler and W. Nazarewicz, Nucl. Phys. A **533**, 249 (1991).